Multispectral mixing scheme for LED clusters with extended operational temperature window

Ming-Chin Chien[1] and Chung-Hao Tien[2,*]

[1]*Department of Photonics and Institute of Electro-Optical Engineering, National Chiao Tung University, 1001 Ta-Hsueh Road, Hsinchu 30010, Taiwan*

[2]*Department of Photonics and Display Institute, National Chiao Tung University, 1001 Ta-Hsueh Road, Hsinchu 30010, Taiwan*

[*]*chtien@mail.nctu.edu.tw*

Abstract: LEDs have changed the concept of illumination not only in an expectation of the highest electroluminance efficiency but also in tremendous chances for smart lighting applications. With a cluster mixing, many studies were addressed to strategically manipulate the chromaticity point, system efficiency and color rendering performance according to different operational purposes. In this paper, we add an additional thermal function to extend the operational thermal window of a pentachromatic R/G/B/A/CW light engine over a chromaticity from 2800K to 8000K. The proposed model is experimentally validated to offer a full operable range in ambient temperature (T_a = 10° to 100°C) associated with high color quality scale (above 85 points) as well as high luminous efficiency (above 100 lm/watt).

OCIS codes: (330.1690) Color; (330.1715) Color, rendering and metamerism; (230.3670) Light-emitting diodes.

References and links

1. G. He and L. Zheng, "Color temperature tunable white-light light-emitting diode clusters with high color rendering index," Appl. Opt. **49**(24), 4670–4676 (2010).
2. G. He and L. Zheng, "White-light LED clusters with high color rendering," Opt. Lett. **35**(17), 2955–2957 (2010).
3. M. C. Chien and C. H. Tien, "Cluster LEDs mixing optimization by lens design techniques," Opt. Express **19**(S4 Suppl 4), A804–A817 (2011), http://www.opticsinfobase.org/oe/abstract.cfm?URI=oe-19-S4-A804.
4. E. F. Schubert, *Light Emitting Diodes*, 2nd ed. (Cambridge University Press, 2006).
5. A. Keppens, W. R. Ryckaert, G. Deconinck, and P. Hanselaer, "Modeling high-power light-emitting diode spectra and their variation with junction temperature," J. Appl. Phys. **108**(4), 043104 (2010).
6. S. Chhajed, Y. Xi, Y. L. Li, T. Gessmann, and E. F. Schubert, "Influence of junction temperature on chromaticity and color rendering properties of trichromatic white light source based on light emitting diodes," J. Appl. Phys. **97**(5), 054506 (2005).
7. Y. Ohno, "Spectral design considerations for white LED color rendering," Opt. Eng. **44**(11), 111302 (2005).
8. K. Man and I. Ashdown, "Accurate colorimetric feedback for RGB LED clusters," Proc. SPIE **6337**, 633702, 633702-8 (2006).
9. F. Reifegerste and J. Lienig, "Modeling of the temperature and current dependence of LED spectra," J. Light Vis. Environ. **32**(3), 288–294 (2008).
10. W. Davis and Y. Ohno, "Color quality scale," Opt. Eng. **49**(3), 033602 (2010).
11. A. Žukauskas, R. Vaicekauskas, and M. S. Shur, "Colour-rendition properties of solid-state lamps," J. Phys. D Appl. Phys. **43**(35), 354006 (2010).
12. Y. Ohno, "Color rendering and luminous efficacy of white LED spectra," Proc. SPIE **5530**, 88–98 (2004).
13. Y. Xi and E. F. Schubert, "Junction-temperature measurement in GaN ultraviolet light-emitting diodes using diode forward voltage method," J. Appl. Phys. **85**, 2163–2165 (2004).
14. Y. Gu and N. Narendran, "A non-contact method for determining junction temperature of phosphor-converted white LEDs," Proc. SPIE **5187**, 107–114 (2004).
15. R. L. Haupt and S. E. Haupt, *Practical Genetic Algorithms*, 2nd ed. (John Wiley, 2004).
16. I. Moreno, M. Avendaño-Alejo, and R. I. Tzonchev, "Designing light-emitting diode arrays for uniform near-field irradiance," Appl. Opt. **45**(10), 2265–2272 (2006).
17. T. Mukai, M. Yamada, and S. Nakamura, "Characteristics of InGaN-based UV/blue/green/amber/red light-emitting diodes," Jpn. J. Appl. Phys. **38**(Part 1, No. 7A), 3976–3981 (1999).
18. Philips Lumileds Lighting Campany, Netherlands, LUXEON Rebel PC Amber Datasheet DS62 (2010).

#159174 - $15.00 USD Received 2 Dec 2011; revised 2 Jan 2012; accepted 3 Jan 2012; published 31 Jan 2012

1. Introduction

Multispectral illumination with multichip LED clusters has the proven potential of revolutionizing the general lighting due to its unique characteristics to strategically modulate the spectral power distribution (SPD) to meet different operational purpose [1, 2]. A new technique, based on the use of general lens design rule to optimize the SPD of a LED cluster, was recently developed at NCTU [3]. This technique was demonstrated to provide the optimal operation with high color quality and efficiency over a wide range of chromaticity. Nevertheless, the assumption of constant thermal environment has prevented to a widespread diffusion of multichip LED clusters, thus precluding its transfer to practical use. In fact, the SPD of a LED more or less has the nonlinear dependence with the junction temperature and drive current, which in turn, results in the performance drift as well as the complexity in spectral modulation. In this study, based on the multispectral mixing scheme, we make an attempt to take the issues of thermal and drive current into consideration. Basically, a successful mixing scheme shall be able to provide two functions:

(a) Estimating the dependence of a LED white composite spectra on the junction temperature and drive current, respectively. Prior works analytically or empirically set either junction temperature or the drive current as the single parameter [1–7]. Although the single-color low power LED spectra in consideration of both temperature and current is available [8, 9], there is still lack of the complete treatment for high power LED, whose model can be simply used to estimate the spectral behavior of phosphor-converted white light.

(b) Formulating the SPD to accommodate an optimization process. A multispectral mixing is a mathematically underdetermined optimization problem. We directly connect tristimulus values with drive current to reduce the degrees of freedom and then incorporate a proposed sampling methodology to find the optimum solution over a range of desired color temperatures [3]. Afterward we complete the optimization process by removing the constraint in ambient temperature to further extend the operable range of the cluster.

The aim of this study is to implement a methodology, with consideration of temperature and drive current, to optimize the SPD of a LED white composite spectra with high color quality and possibly highest efficiency in a defined range of chromaticity. In this paper, we use color quality scale (CQS) as the merit figure of the light quality [10]. Interested readers can refer to ref [11] for more discussion about color appearance and perceptual difference by various qualitative characteristics of lighting. In terms of system efficiency, we employ a factor: luminance efficiency (LE), where LE is defined as how much luminous flux (lm) normalized to the electrical input power (watt) expended to operate the LED [12].

2. Measurement and modeling

2.1 Spectral measurement

In order to characterize the spectral property, we firstly launch the pulsed calibration measurement to obtain the database of forward voltage (V_f) subject to a set of two parameters: junction temperatures (T_j) and pulsed drive current (I_d), respectively [13]. The sample LED is mounted inside an oven with every 10°C temperature increment. The junction temperature is assumed to be equivalent to oven temperature under the assumption that no additional thermal effect is induced by pulsed current with low duty cycle [14]. For each drive current, a calibration curve that profiles the relationship between the forward voltage V_f and junction temperatures T_j can be expressed by a linear estimation as shown in Eq. (1):

$$T_j \cong \frac{T_2 - T_1}{V_f(T_2) - V_f(T_1)}[V_f - V_f(T_1)] + T_1 \quad (1)$$

#159174 - $15.00 USD Received 2 Dec 2011; revised 2 Jan 2012; accepted 3 Jan 2012; published 31 Jan 2012

where T_1 = 10 °C and T_2 = 100 °C represent the extreme two cases as the thermal boundary. Afterward, a DC current (I_{DC}) is applied through the sample LED mounted on a fixture (Arroyo Instruments, TEC 264-BB-DB9). The entire module is placed inside the cavity of an integrating sphere. The temperature of the fixture controlled by a thermoelectric cooler (Arroyo Instruments, TEC Source 5310) can be selected as the ambient temperature (T_a). With a set of ambient temperature (T_a) and DC current (I_{DC}), as well as junction temperatures (T_j) and pulsed drive current (I_d), the emitted SPD of each sample LED can be measured by the spectrometer (SR-UL1R, Topcon) attached to the integrating sphere. As the thermal states reach to the stable status, the junction temperature (T_j) can be determined by the interpolation mapping of the forward voltage according to the pulsed calibration measurement.

Based on a finite set of measurements, we could have the database $\mathbf{S}\{\mathbf{t_j}, \mathbf{i_{DC}}\}$ that serves as a foundation for the spectral modeling and the database $\mathbf{S}\{\mathbf{t_a}, \mathbf{i_{DC}}\}$ would be used to simplify the optimization process, respectively. Through this paper, vectors are denoted by bold-faced lower-case letters, e.g., $\mathbf{t_j}$ (junction temperature), $\mathbf{i_{DC}}$ (DC drive current). Matrices are represented by bold-faced capital letters, e.g., **S** (SPD of sample LED). Where **S** is an M x N matrix representing the M recorded spectra (here M = 100) uniformly sampled by N points (N = 40, 380nm to 780nm in steps of 10nm). Each row of the **S** contains one synthesized SPD of denoted as **s**. The $\mathbf{t_j}$, $\mathbf{t_a}$ and $\mathbf{i_{DC}}$ are M x 1 vectors indicating M modulations of T, T_a, and I. It's likely to link T_a to T_j so that the thermal resistance R_t between the junction and the reference point can be determined by Eq. (2):

$$R_t = \frac{T_j - T_a}{P_e - \Phi} \tag{2}$$

where the denominator, the difference of the input electric power P_e and the radiant flux Φ, indicates the power dissipated in the LED.

2.2 Spectral modeling

Generally, the SPD can be fitted by a single Gaussian function, which incorporates three parameters, the spectral power (P), peak wavelength (λ_0) and spectral width ($\Delta\lambda$) with junction temperature [4]. However, in most of cases, SPD is not perfectly symmetric, which would lead to numerical error by single Gaussian fitting. In order to overcome this issue, in this study, we proposed a double Gaussian function with two sets of parameters: $(P, \lambda_0, \Delta\lambda)$ and $(P', \lambda_0', \Delta\lambda')$. All the parameters are functions of both junction temperature and drive current. The estimated M x N spectral matrix $\tilde{\mathbf{S}}$ for a single-color LED can be modeled as Eq. (3):

$$\tilde{\mathbf{S}} = \mathbf{G} + \mathbf{G'} \tag{3}$$

where $\mathbf{G} = (\mathbf{g_1}, \ldots, \mathbf{g_M})^{\mathbf{T}}$ and $\mathbf{G'} = (\mathbf{g'_1}, \ldots, \mathbf{g'_M})^{\mathbf{T}}$ are Gaussian spectral matrices. Here we temporarily omit $\mathbf{G}'$ due to the same treatment from Eqs. (4)–(6). The matrix **G** has M spectral vectors **g** with N sampling wavelengths. For the nth point of mth row vector $\mathbf{g_m}$, g_{mn}, its value can be accounted by Eq. (4):

$$g_{mn} = p_m \exp\{-[\lambda_n - (\lambda_0)_m]^2 / \Delta\lambda_m^2\} \tag{4}$$

The parameters p_m, $(\lambda_0)_m$, and $\Delta\lambda_m$ refer to the mth power, peak wavelength, and spectral width, whose values could be found by satisfying the minimization of Eq. (5):

$$\arg\min[|\mathbf{s_m} - \tilde{\mathbf{s}}_\mathbf{m}|^2, \{p_m, (\lambda_0)_m, \Delta\lambda_m, p'_m, (\lambda_0')_m, \Delta\lambda'_m\}] \tag{5}$$

where $\mathbf{s_m}$ and $\tilde{\mathbf{s}}_\mathbf{m} = \mathbf{g_m} + \mathbf{g'_m}$ are the mth row vectors of **S** and $\tilde{\mathbf{S}}$, respectively. After solving whole rows we have three M x 1 vectors **p**, $\boldsymbol{\lambda_0}$, and $\boldsymbol{\Delta\lambda}$ that can empirically be related to $\mathbf{t_j}$ and $\mathbf{i_{DC}}$ as shown in Eq. (6):

#159174 - $15.00 USD Received 2 Dec 2011; revised 2 Jan 2012; accepted 3 Jan 2012; published 31 Jan 2012

$$\ln(\mathbf{p}) = \mathbf{M}_{\mathbf{p}}\mathbf{c}_{\mathbf{p}}, \boldsymbol{\lambda}_0 = \mathbf{M}_{\boldsymbol{\lambda}}\mathbf{c}_{\boldsymbol{\lambda}}, \text{and} \ln(\boldsymbol{\Delta\lambda}) = \mathbf{M}_{\boldsymbol{\Delta\lambda}}\mathbf{c}_{\boldsymbol{\Delta\lambda}} \quad (6)$$

where $\mathbf{M}_{\mathbf{p}} = [\mathbf{t}_{\mathbf{j}}^{\mathrm{T}} \ln(\mathbf{t}_{\mathbf{j}}) \ln(\mathbf{i}_{\mathbf{DC}}) \mathbf{l}]$, $\mathbf{M}_{\boldsymbol{\lambda}} = [\mathbf{t}_{\mathbf{j}} \ln(\mathbf{i}_{\mathbf{DC}}) \mathbf{l}]$ and $\mathbf{M}_{\boldsymbol{\Delta\lambda}} = [\mathbf{t}_{\mathbf{j}} \ln(\mathbf{t}_{\mathbf{j}})^{-1} (\mathbf{i}_{\mathbf{DC}})^{1/2} \mathbf{l}]$ are all M x 3 basis matrices. $\mathbf{l}$ indicates the M x 1 all-ones vector. $\mathbf{c}_{\mathbf{p}}$, $\mathbf{c}_{\boldsymbol{\lambda}}$, and $\mathbf{c}_{\boldsymbol{\Delta\lambda}}$ represent 3x1 coefficient vectors, whose values could be calculated by linear least square method, e.g. $\mathbf{c}_{\mathbf{p}} = \left(\mathbf{M}_{\mathbf{p}}^{\mathrm{T}}\mathbf{M}_{\mathbf{p}}\right)^{-1}\mathbf{M}_{\mathbf{p}}^{\mathrm{T}} \ln\left(\mathbf{p}\right)$. Appling the above regularized process to G' will lead to the other set of coefficient vectors $\left(\mathbf{c}_{\mathbf{p}}', \mathbf{c}_{\boldsymbol{\lambda}}', \mathbf{c}_{\boldsymbol{\Delta\lambda}}'\right)$. Thus, the complete function $\tilde{S}(\lambda)$ for single-color LED spectrum at junction temperature T_j and drive current I_{DC} can be expressed as Eq. (7):

$$\begin{aligned} \tilde{S}(\lambda) &= G + G' \\ &= \exp[\mathbf{m}_{\mathbf{p}}\mathbf{c}_{\mathbf{p}} - (\lambda - \mathbf{m}_{\boldsymbol{\lambda}}\mathbf{c}_{\boldsymbol{\lambda}})^2 / \exp(\mathbf{m}_{\boldsymbol{\Delta\lambda}}\mathbf{c}_{\boldsymbol{\Delta\lambda}})^2] \\ &+ \exp[\mathbf{m}_{\mathbf{p}}\mathbf{c}_{\mathbf{p}}' - (\lambda - \mathbf{m}_{\boldsymbol{\lambda}}\mathbf{c}_{\boldsymbol{\lambda}}')^2 / \exp(\mathbf{m}_{\boldsymbol{\Delta\lambda}}\mathbf{c}_{\boldsymbol{\Delta\lambda}}')^2] \end{aligned} \quad (7)$$

where $\mathbf{m}_{\mathbf{p}} = [T_j \ln(T_j) \ln(I_{DC}) 1]$, $\mathbf{m}_{\boldsymbol{\lambda}} = [T_j \ln(I_{DC}) 1]$, and $m_{\Delta\lambda} = [T_j \ln(T_j)^{-1} (I_{DC})^{1/2} 1]$ account for basis vectors with free variables T_j and I_{DC}, respectively. Figure 1 illustrates the double Gaussian model for green and phosphor-converted LED emission spectra at T_j = 25°C and I_{DC} = 350mA, respectively.

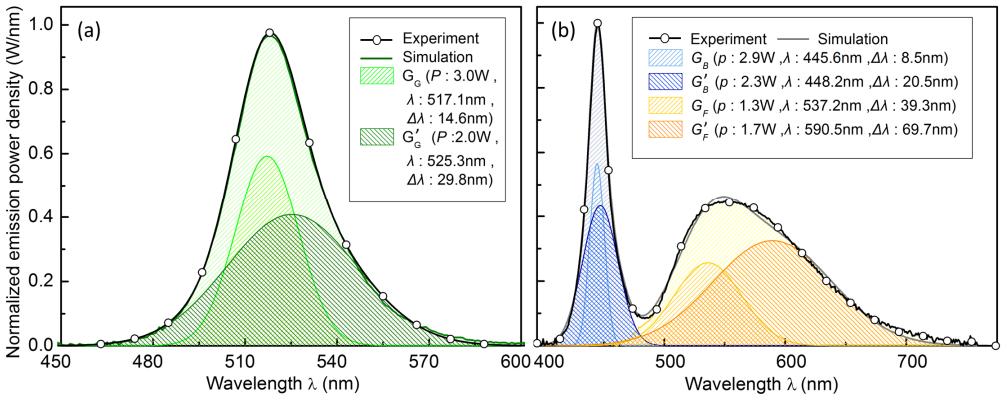

Fig. 1. The illustration of double Gaussian model for green and phosphor LED spectra at T_j = 25°C and I_{DC} = 350mA respectively. For the phosphor-converted LEDs, the blue and fluorescence components should be individually considered, thus decomposed into two double Gaussian functions G_B + G_B' and G_F + G_F', respectively. The numerical model Eqs. (3)–(7) ensure a good approximation at arbitrary junction temperature T_j and drive current I_{DC}.

For the phosphor-converted white LED $\tilde{S}_{\mathrm{W}}(\lambda)$, the estimated spectrum is composed of two double Gaussian functions as given by Eq. (8):

$$\tilde{S}_W(\lambda) = \begin{cases} G_B + G_B', & for\ \lambda < \lambda_{BF} \\ G_F + G_F', & for\ \lambda > \lambda_{BF} \end{cases} \quad (8)$$

where λ_{BF} denotes the boundary in the middle of blue ($G_{\mathrm{B}} + G_{\mathrm{B}}'$) and fluorescence ($G_{\mathrm{F}} + G_{\mathrm{F}}'$) component.

The spectral modeling of each component functions G_{B}, G_{B}', G_{F}, and G_{F}' follows the same mathematical manipulation as single-color case, shown in Eqs. (3)–(7). A good agreement between the experimental measurement and spectral model can be obtained with R^2 exceeding 0.98.

#159174 - $15.00 USD Received 2 Dec 2011; revised 2 Jan 2012; accepted 3 Jan 2012; published 31 Jan 2012

3. Optimization

3.1 Optimization process

The problem of color render is crucial when we are able to reproduce sources with different SPDs but equal correlated color temperature (CCT) (and even chromaticity). Such metameric will provide different CIE tristimulus values for a reflecting test sample if illuminated with one source or the other. In terms of LEDs cluster (K-type LED emitters, usually K > 3), metamerism appears as the SPD is synthesized for a target tristimulus value $\varepsilon = [X\ Y\ Z]^{T}$. Before manipulating of SPD toward the target value, the current tristimulus value $\tilde{\boldsymbol{\varepsilon}}$ can be described as Eq. (9):

$$\tilde{\boldsymbol{\varepsilon}} = \mathbf{A}\tilde{\mathbf{S}}^{\mathbf{T}}\mathbf{l} \tag{9}$$

where rows of $\mathbf{A}$ are the sampled color matching functions with dimension N, the K x N spectral matrix $\tilde{\mathbf{S}}$ now contains K-type modeled spectra [from Eq. (7) or Eq. (8)] extracted N discrete points, and $\mathbf{l}$ becomes the K x 1 all-ones vector. In this system, two implicit free variables junction temperature (T_j) and drive current (I_{DC}) make the degrees of freedom to be $2K$–3, results in the computational complexity to optimize the operational condition: the possibly highest objective function (included luminous efficiency and light quality) in a predefined chromaticity point ε. To solve this issue, we impose a constraint on a localized area (with small number of LEDs), where the ambient temperature T_a is assumed to be uniform among this area. Therefore the junction temperature T_j for each type LED can be determined by Eq. (2) once T_a and I_{DC} are given. Such assumption, however, degenerates the degrees of freedom $2K$–3 into K–3 + 1. On the other hand, we tend to directly relate the tristimulus value to drive current to further simplify the optimization process. We find a quadratic current basis $\mathbf{i_{DC}} = [1\ (I_{DC})_1\ (I_{DC})_1^{\,2}\ (I_{DC})_2\ (I_{DC})_2^{\,2} \cdots (I_{DC})_k\ (I_{DC})_k^{\,2}]^{\mathbf{T}}$ can precisely characterize $\tilde{\boldsymbol{\varepsilon}}$ under a specific T_a. In sum, the Eq. (9) can be rewritten as Eq. (10) with lower degrees of freedom:

$$\tilde{\boldsymbol{\varepsilon}} = \mathbf{C}^{\mathbf{T}}\mathbf{i_{DC}} \tag{10}$$

where $\mathbf{C}$ is $(2K + 1)$ x 3 coefficient matrix. Now we force current tristimulus to be equal to a target tristimulus $\tilde{\boldsymbol{\varepsilon}} = \boldsymbol{\varepsilon}$ and randomly choose values for K–3 currents. An arbitrary current combination will readily be produced by extracting the positive solutions for remained currents. An initial current population, $\mathbf{I_{DCp}}$, of "combination changes" with various drive current could be generated. The corresponding initial $\mathbf{T_j}$ population, $\mathbf{T_{jP}}$, is obtained by introducing $\mathbf{I_{DCp}}$ and T_a to Eq. (2). Similarly, the initial SPD population, $\tilde{\mathbf{S}}_{\mathbf{P}}$, comes out via bringing the corresponded T_j and I_{DC} from $\mathbf{T_{jP}}$ and $\mathbf{I_{DCp}}$ into Eq. (7) or (8) for single-color or phosphor-converted LEDs, respectively.

To evaluate the performance of the combinations in $\tilde{\mathbf{S}}_{\mathbf{P}}$, based on the weighted sum method, we introduce Eq. (11) as a user-defined merit function (or called objective function) with two figures of merit: luminous efficiency (LE) and color quality scale (CQS), respectively:

$$f = w \times CQS + (1 - w) \times LE,\ \ subject\ to\ w \in [0,1] \tag{11}$$

where w represents the weight factor for different operational purposes. As we insert each combination of $\tilde{\mathbf{S}}_{\mathbf{P}}$ into Eq. (11), a table of objective values becomes a function of SPD population $\tilde{\mathbf{S}}_{\mathbf{P}}$, or equivalently, a function of $\mathbf{I_{DCp}}$. After defining the correspondence between the merit function and SPD, we bring the table into a globe searching engine, continuous genetic algorithm (CGA), to achieve an improved spectral synthesizing [15]. In the CGA, each row of the table composed of a value of merit function and the associated drive current

#159174 - $15.00 USD Received 2 Dec 2011; revised 2 Jan 2012; accepted 3 Jan 2012; published 31 Jan 2012

combination is regarded as a chromosome. The chromosomes are ranked based on the value of merit function under a process of natural selection. The survivors are deemed fit enough to mate and to afford new offspring. By multiplying a certain mutation rate into the total number of drive currents, we are able to avoid the predicament of overly fast convergence or trapped at a local limitation. Finally, the described process is iterated for several generations until the convergence requirement is satisfied.

3.2 Merit analysis

Another aspect that must be taken into account in the frame work of realizing a smart lighting is the selection of weight factor *w*. Up to this point, a system with a user-defined merit function has been discussed. The weight factor, w, is then used to provide a freedom to determine the operational mode. When $w = 0$, the system is carried out in high efficiency mode, the objective function is entirely attributed to the efficiency consideration. The other extreme case ($w = 1$) would be high quality mode. In most of case, the user-defined intermediate value would be the kernel of the smart lighting operation. Also, Eq. (11) constitutes a two-dimensional optimal boundary (Pareto front, PF) between CQS and LE, respectively. Different weight values *w* would profile a series of locus of operating point. For the sake of computation efficiency, we adapt the proposed sampling methods to analyze the cluster performance among the CQS and LE and produce an appropriate value *w* if any section of PF fulfilled the required performance [3].

4. Design example

A direct experimental validation of the devised model is pursued. A pentachromatic mixing scheme is setup, where a high-power LEDs clusters is composed of four single-colors red/amber/green/blue (R/A/G/B) and a phosphor-converted cool-white (CW) LED. All the chips are commercially available (HELIO Optoelectronics Corp., HMHP-E1LW). Figure 2 shows the SPD of each channel under operational condition T_a = 10°C and I_{DC} = 350mA, respectively. An adequate layout of LED pixel arrangement and first-order design delivers a uniform illumination upon the test Macbeth color checker [16].

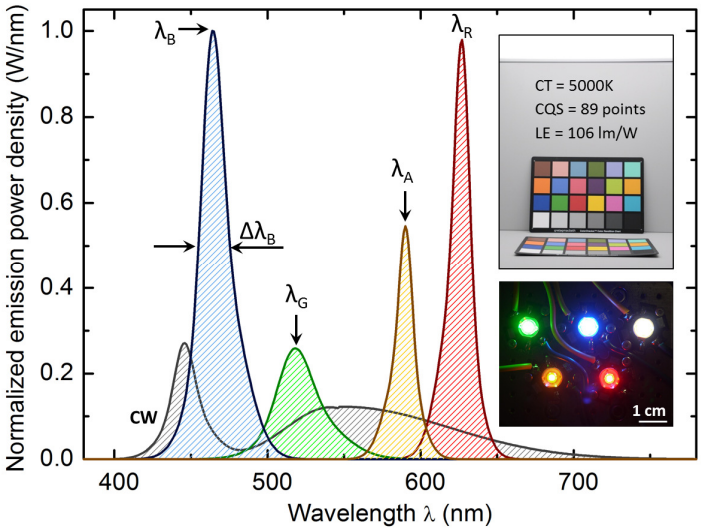

Fig. 2. The power spectra of red (λ_R: 625nm, $\Delta\lambda_R$: 20nm), green (λ_G: 523nm, $\Delta\lambda_G$: 33nm), blue (λ_B: 465nm, $\Delta\lambda_B$: 25nm), amber (λ_A: 587nm, $\Delta\lambda_A$: 18nm) and cool-white LEDs at T_a of 10°C with I_{DC} of 350mA. The upper right figure shows a real-field test designed for CT = 5000K and the lower right one shows the utilized LEDs attached on the temperature controllable fixture respectively.

#159174 - $15.00 USD Received 2 Dec 2011; revised 2 Jan 2012; accepted 3 Jan 2012; published 31 Jan 2012

The first validation of the devised model is conducted by examining the temperature dependence of spectra under four color temperatures: CT = 3200K, 4600K, 6200K, and 7400K, respectively. The system is operated under a specific value of the ambient temperature, T_a = 50°C. The results are reported in Fig. 3, where the illumination conditions fulfill the requirements of high luminance level (100 lm), negligible color deviation (Δxy < 0.01) and high quality (CQS > 85 points) with possibly highest luminous efficiency (LE). If we change the ambient temperature without compensation, the lighting performance would dramatically shift due to the thermal effects. Taking CT = 3200K for example, as ambient temperature increases from 10 °C to 100 °C, the chromaticity point would have an apparent change (Δxy > 0.5). On the other hand, in case of settled operational ambient temperature T_a = 50°C, the acceptable tolerance (Δxy < 0.01) of thermal dependence merely lie in a tiny window T_a = 42 °C ~56 °C. It is observed that the operational window changes with respect to different chromaticity points. The drift of chromaticity point subject to thermal dissipation becomes more severe at low CT, which is mainly attributed by amber and red color. The reason can be explained by Fig. 4.

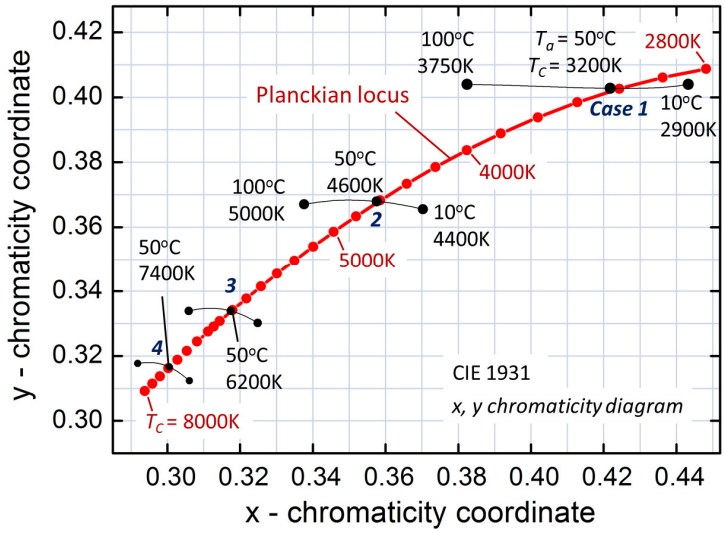

Fig. 3. The temperature dependence of spectra designed for CT = 3200K, 4600K, 6200K, and 7400K at T_a = 50°C. The chromaticity point shifts toward higher color temperature with the raise of T_a owing to the dramatic deterioration in LEs of the red and amber LEDs.

When the ambient temperature T_a increases to 100 °C, luminous efficiencies (LEs) of amber and red LED suffer from 23% and 46% decreases of those at 10 °C, respectively. The results is in agreement with the previous literature, experimentally validated the output power decreases by increasing ambient temperature [17]. The results can be attributed to two reasons: (1) In viewpoint of spectral characteristics, at high ambient temperature T_a, the SPDs of amber and red color would shift to longer wavelength, result in the decreases of luminous efficiency [13]. (2) In terms of material, for the AlInGaP-based LEDs, due to the carrier overflow by increased ambient temperature, the luminous efficiency would be reduced accordingly [17]. In order to compensate the operational shift by thermal effects, a proposed compensation scheme shall be included. The outcomes are summarized in Table 1.

#159174 - $15.00 USD Received 2 Dec 2011; revised 2 Jan 2012; accepted 3 Jan 2012; published 31 Jan 2012

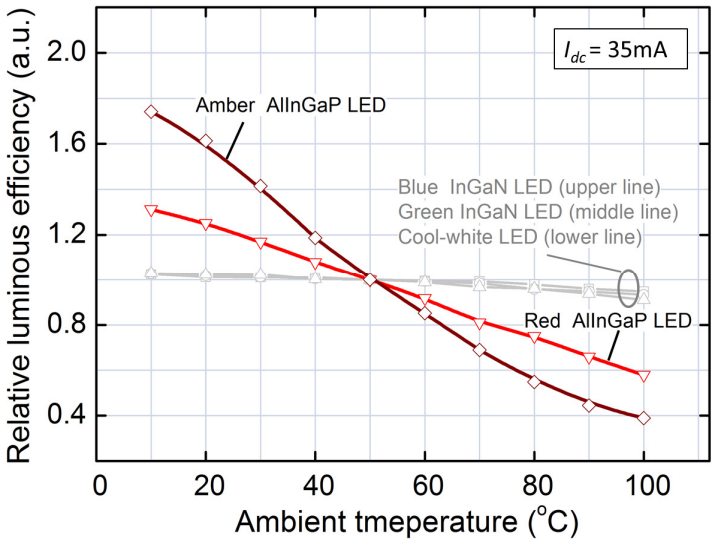

Fig. 4. The temperature dependence of LE for pentachromatic LEDs. When T_a is varied from 10 °C to 100 °C, LEs of amber and red AlInGaP LEDs decrease to 23% and 46% of that at 10 °C while LEs of InGaP LEDs are insensitive to temperature variation.

It is observed that the technique effectiveness is fully applied for the predefined requirements in smart lighting: high color quality scale (above 85), high luminous efficiency (above 100 lm/watt) over a wide range of color temperature (CT = 2800-8000K). The thermal compensation technique works with wide chromaticity locus and, in particular, it is proven to work with low color temperature noticeably influenced by thermal variation. Taking case I (CT = 3200K) for example, as the ambient temperature T_a changes from 10 °C to 100 °C, the power ratio of dominant red channel changes from 28% to 44%. The reason is due to when ambient temperature increases the luminous efficiency (LE) of dominant field (Red color) decreases. In order to keep the chromaticity point, we must extract more luminous flux from the red majority and thus more power ratio (P_{in}) is required accordingly. The consequence can be deduced in other operational conditions. As the lighting is operation at high color temperature (CT > 4600K), phosphor-converted white source is the dominant field (over 50%) due to its unique characteristics of high luminous efficiency and dully dependence upon the thermal effects. Therefore, in case of operation in high color temperature (CT), we suggest a scenario as following: (1) utilize phosphor-converted white source as a dominant field, accompanied by a small amount of other complementary single-color to keep light quality and fine chromaticity adjustment, (2) replace single red and amber emitters by two or more devices with less drive current, and thus reduce the thermal effect and enhance the entire cluster efficiency, (3) replace amber AlInGaP LED by phosphor-converted amber with higher flux density and better color stability [18].

#159174 - $15.00 USD Received 2 Dec 2011; revised 2 Jan 2012; accepted 3 Jan 2012; published 31 Jan 2012

Table 1. The Comparison of CQS, LE, Output Spectral Power *P*, Correlated Color Temperature CCT, Color Temperature CT and the Input Power Ratio P_{in} under T_a = 10°C, 50°C and 100°C

	Case	1	2	3	4
10°C	CCT(K)	2900	4400	6100	7300
	CQS	86	89	87	86
Simulation	LE(lm/watt)	123	131	130	127
(w/o compensation)	P(lm)	127	114	110	109
	CT (K)	3200	4600	6200	7400
	CQS	89	91	90	88
Simulation	LE (lm/W)	127	131	130	127
(with compensation)	P(lm)	100	100	100	100
	P_{in} (%)	28:24:0:26:22 R:A:G:B:CW	14:17:3:24:42	7:12:8:21:52	5:10:12:20:53
	CCT (K)	3168	4538	6145	7327
Measurement	CQS	88	90	89	88
	LE (lm/W)	124	128	128	125
	P (lm)	96	97	96	96
50°C	CT (K)	3200	4600	6200	7400
	CQS	90	89	89	87
Simulation	LE (lm/W)	109	123	124	123
	P(lm)	100	100	100	100
	P_{in} (%)	33:23:0:23:21	17:17:2:21:43	5:12:7:18:58	5:9:11:16:59
	CCT (K)	3226	4631	6170	7365
Measurement	CQS	88	88	87	86
	LE (lm/W)	105	118	120	120
	P (lm)	95	94	96	95
100°C	CCT(K)	3750	5000	6600	7700
	CQS	77	86	87	87
Simulation	LE(lm/watt)	82	103	111	110
(w/o compensation)	P(lm)	74	84	88	89
	CT (K)	3200	4600	6200	7400
	CQS	87	87	87	87
Simulation	LE (lm/W)	62	92	109	107
(with compensation)	P(lm)	100	100	100	100
	P_{in} (%)	44:24:0:18:14	11:28:1:19:41	1:15:3:11:70	1:12:9:12:66
	CCT (K)	3252	4687	6253	7439
Measurement	CQS	86	85	86	86
	LE (lm/W)	59	87	105	104
	P (lm)	95	95	95	97

In sum, Fig. 5 shows the contour map of possibly highest luminous efficiency (LE) subject to predefined requirements (CQS > 85 points, high luminance level 100 lm and negligible color deviation $\Delta xy < 0.01$). With different operational ambient temperatures, it's not likely to reach high efficiency at high ambient temperatures. The best performance (LE > 130 lm/W) lies in a narrow region about CT = 4000-6500K associated with self-evident low ambient temperature (T_a = 10 °C ~20 °C). If the LE = 100 lm/W is settled as the minimum requirement, a full operable range for T_a is workable only exists in high color temperature CT > 5200K.

#159174 - $15.00 USD Received 2 Dec 2011; revised 2 Jan 2012; accepted 3 Jan 2012; published 31 Jan 2012

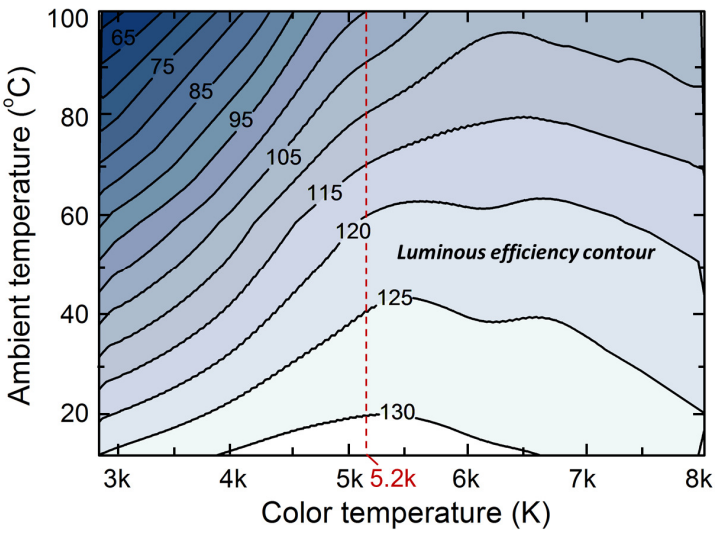

Fig. 5. The LE contour of the pentachromatic LEDs cluster is performed under the predefined requirements (CQS > 85 points, lighting level = 100 lm and Δxy < 0.01). When the LE = 100 lm/W is selected as the minimum efficiency boundary, a full operation range for ambient temperature can be obtained for CT > 5200K.

4. Conclusion

A through methodology, which takes into account all aspects which can have influence on general lighting, has been firstly developed and experimentally validated. Firstly, a double Gaussian fitting is proposed to precisely describe the SPD of either phosphor-converted or single-color LEDs. Then we employ a user-define merit function to optimize the SPD of a LEDs cluster without loss of generality. In the optimization process, the degrees of freedom can be reduced from $2K-3$ to $K-2$ under the localized uniform T_a. The optimal spectral synthesis can be completed by incorporating CGA and Tien's method [3]. In order to validate the proposed scheme, we set up a pentachromatic R/G/B/A/CW cluster. At high ambient temperature T_a, the luminous efficiency would suffer from a severe deterioration at low color temperature. The main reason is due to the dominant fields, red and amber, are strongly dependent on thermal dissipation. In order to avoid such case, we suggest replacing single emitter by two or more ones, which are able to share the total luminous flux and reduce the thermal effect accordingly. This technique still leaves much space open and clearly more research must be carried out to explore its potential in full- the first, price and volume of the cluster being the realization of a commercial available solution. The preliminary demonstration presented here, however, indicate that proposed multispectral mixing scheme could create a major breakthrough in the field of general lighting and spectral technologies.

Acknowledgment

We appreciate the financial support provided by the National Science Council, Taiwan, under grants NSC 99-2221-E-009-067-MY3 and NSC 100-2622-E-009-003-CC2.

#159174 - $15.00 USD Received 2 Dec 2011; revised 2 Jan 2012; accepted 3 Jan 2012; published 31 Jan 2012